Correspondence imaging based on correlation coefficients

Xuri Yao (姚旭日)[1,2], Xuefeng Liu (刘雪峰)[1,2], Wenkai Yu (俞文凯)[1,2], and Guangjie Zhai (翟光杰)[1*]

[1]*Key Laboratory of Electronics and Information Technology for Space Systems, Center for Space Science and Applied Research, Chinese Academy of Sciences, Beijing 100190, China*

[2]*University of Chinese Academy of Sciences, Beijing 100049, China*

[*]*Corresponding author: gjzhai@nssc.ac.cn*

Received August 10, 2014; October 24, 2014; posted online December 30, 2014

In the context of correspondence ghost imaging, we utilize the correlation coefficients to separate the reference detector speckle patterns into positive and negative correlated parts. A positive image and a negative image of the object are obtained by averaging over corresponding speckle patterns. The visibility and contrast-to-noise ratio of the positive image are discussed, and it is found that the latter will reach a maximum by averaging over a little less than half of the total number of reference speckle patterns.

OCIS codes: 030.0030, 030.6140.
doi: 10.3788/COL201513.010301.

Ghost imaging (GI) has attracted great interest in the past decade due to its nonlocal nature. In conventional GI, two spatially coherent light beams are used, one is a signal beam and the other a reference beam. The former illuminates an object and is collected by a so-called "bucket detector," which has no spatial resolution and measures only the total transmitted/reflected intensity. The reference beam that does not illuminate the object is measured by a pixel array detector which has spatial resolution. The image of the object is reconstructed through spatial intensity correlation measurements. The first ghost image was achieved with entangled biphoton pairs generated by spontaneous parameter down-conversion[1]; and later, theoretical and experimental studies showed that classical light can also be used to perform GI[2–8]. Since then, many improved versions of GI have appeared, such as computational GI[9], differential GI[10], and GI via sparsity constraints[11]. However, they all have certain shortcomings, in particular, long data accumulation and processing time measurement time due to the second-order correlation computation on which they are based.

Recently, a novel GI scheme called correspondence imaging (CI)[12,13] was demonstrated by Luo *et al.* in which the intensity values of the bucket detector are sorted and divided into two parts relative to the mean. The reference speckle patterns are divided correspondingly into two parts. A positive image and a negative image of the object are produced by averaging the respective speckle patterns instead of correlation calculations. In this way, the computation time can be greatly reduced while the visibility and signal-to-noise ratio (SNR) are much improved, especially for the negative image. Although the theoretical explanation of this phenomenon is still under debate, it has already been used for improving the quality of GI[14,15]. It is well-known that the GI performance grows better as the intensity fluctuation increases, but the "anti-correlation" shown in the negative image is quite counterintuitive.

In this letter, we use the correlation coefficients to explain the production of the positive and the negative images, and show that the mean of the bucket detector signals is not a necessarily best boundary to divide the reference speckle patterns. An image reconstruction scheme based on the statistical average is presented, which agrees well with the simulation results. We also investigate the visibility and contrast-to-noise ratio (CNR)[16] of images, and show that the CNR will reach a maximum when the number of reference patterns to be averaged over is less than half of the total. This approach also has the benefits of high SNR, less data, and simpler computation.

The basic setup for lensless GI is shown in Fig. 1. The field from a thermal or a pseudothermal light source is separated by a beam splitter into two identical beams. In the signal arm, the light passes through the object to be collected by a bucket detector. In the reference arm, a detector with spatial resolution records the speckle pattern, at the same distance from the source as the object. In each exposure, the total intensity collected by the bucket detector is

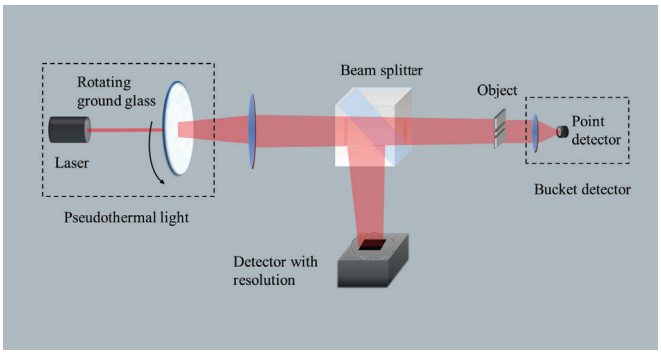

Fig. 1. Experimental setup of lensless GI.

$$I_B^{(i)} = \sum_x I_R^{(i)}(x) O(x), \tag{1}$$

where $I_R^{(i)}(x)$ is the speckle pattern on the reference plane for the ith measurement, $O(x)$ is the transmission function of the object. After a total of M measurements, the image can be obtained from the second-order correlation

$$G(x) = \frac{1}{M} \sum_{i=1}^{M} I_B^{(i)} I_R^{(i)}(x). \tag{2}$$

In imaging processes, a correlation coefficient is commonly used to evaluate the comparability of two images[17], which are usually expressed by matrices. The correlation coefficient between two matrices A and B is defined as

$$\rho = \frac{\sigma(A,B)}{\sqrt{\sigma_A^{\,2}\sigma_B^{\,2}}}, \tag{3}$$

where $\sigma(A, B)$ is the covariance between A and B, and σ_A^2 and σ_B^2 are the variances of A and B, respectively. The correlation coefficient has a range of values from −1 to 1, and 0 is the boundary between positive and negative correlations. If $0 < \rho < 1$, A and B show a positive correlation, which means A is similar to B, and if $-1 < \rho < 0$, A and B show a negative correlation, which means A is similar to B but with its gray value inversed. The correlation coefficient ρ will have a maximum value of 1 when A can be expressed as a linear function of B.

Substituting Eq. (1) and the transmission function of the object $O(x)$ into Eq. (3), we obtain the correlation coefficient between the object transmission function and the speckle pattern recorded in the reference arm for the ith measurement

$$\rho_{I_R^{(i)}O} = \frac{\frac{1}{N}\sum_x I_R^{(i)}(x)O(x) - \frac{1}{N}\sum_x I_R^{(i)}(x)\frac{1}{N}\sum_x O(x)}{\sqrt{\sigma^2_{I_R^{(i)}(x)}\sigma_o^{\,2}}}, \tag{4}$$

where N is the total number of pixels that the object would cover on the reference detector. The speckle patterns produced by thermal light or pseudothermal light obey a negative exponential intensity distribution, in which the relationship between the variance and the average intensity of the speckle pattern is[18]

$$\sigma^2_{I_R^{(i)}(x)} = \overline{I_R^{(i)}}^{\,2}, \tag{5}$$

where $\overline{I_R^{(i)}} = \frac{1}{N}\sum_x I_R^{(i)}(x)$ is the average intensity of the speckle pattern $I_R^{(i)}(x)$. Consequently, the correlation coefficient between the object transmission function and the speckle pattern is given by

$$\rho_{I_R^{(i)}O} = \frac{\frac{1}{N}\left(I_B^{(i)} - N\overline{I_R^{(i)}}T\right)}{\overline{I_R^{(i)}}\sqrt{\sigma_o^{\,2}}}, \tag{6}$$

where $T = \frac{1}{N}\sum_x O(x)$ is the transmission ratio of the object. The above expression shows that the correlation coefficient is determined by the bucket detector signal $I_B^{(i)}$. If $I_B^{(i)} > N\overline{I_R^{(i)}}T$, the speckle pattern is positively correlated with the object, and if $I_B^{(i)} < N\overline{I_R^{(i)}}T$, it is negatively correlated with the object.

From Eq. (1), it can be seen that GI is a process of weighted averaging, and the positive correlated speckle patterns share bigger weights, so the negative correlated speckle patterns are merged in the background and a positive image emerges. But if we divide the speckle patterns into two parts according to the sign of the correlation coefficients and calculate the intensity correlations separately, then we can obtain both positive and negative GIs. The numerical simulation results are shown in Fig. 2 for a digital object "NSSC," which is 300×300 pixels in size with three gray scales (Fig. 2(a)). The image reconstructed by correlation calculations with all the speckle patterns is shown in Fig. 2(b); the positive and negative images reconstructed by correlation calculations with the speckle patterns separated by correlation coefficients are shown in Figs. 2(c) and (d), respectively. The total number of measurements is taken to be 120000.

We now describe how a positive or a negative image can be obtained just by averaging over the speckle patterns which are correlated either positively or negatively with the object, with no correlation calculation needed. We treat the positively correlated speckle pattern as a linear function of the object mixed with noise.

$$I_{R+}^{(i)}(x) = kO(x) + e(x), \tag{7}$$

where the subscript + denotes positive correlation, k is a proportionality coefficient, and $e(x)$ is the noise. Suppose the noise at different pixels is independent and identically distributed. The standard variance of the

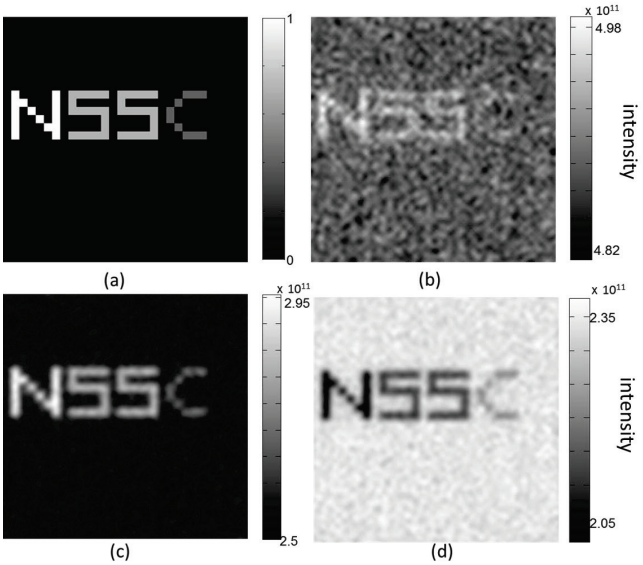

Fig. 2. Numerical simulation of positive GI and negative GI: (a) object, (b) conventional GI, (c) positive GI, and (d) negative GI.

noise will decrease with the number of measurements according to

$$\sigma_e' = \sqrt{\frac{1}{M}}\sigma_e, \tag{8}$$

where σ_e and σ_e' are the standard variances of the noise at a pixel before and after averaging, respectively. Thus, the process of speckle pattern averaging can be seen as a process of noise elimination. After averaging the positively correlated speckle patterns, the noise at different pixels should become a uniform background so we can obtain

$$\left\langle I_{R+}^{(i)}(x)\right\rangle = kO(x) + \left\langle e\right\rangle, \tag{9}$$

where $\left\langle I_{R+}^{(i)}(x)\right\rangle = \frac{1}{M_+}\sum_{i=1}^{M+} I_{R+}^{(i)}(x)$, M_+ is the total number of the positively correlated patterns and $\left\langle e\right\rangle$ is the expected value of the noise. We then obtain the relation

$$\left\langle I_{B+}^{(i)}\right\rangle = TN\left(k + \left\langle e\right\rangle\right), \tag{10}$$

where $\left\langle I_{B+}^{(i)}\right\rangle = \frac{1}{M_+}\sum_{i=1}^{M+} I_{B+}^{(i)}$ is the mean of bucket detector signals which show positive correlations, and

$$\overline{\left\langle I_{R+}^{(i)}\right\rangle} = Tk + \left\langle e\right\rangle, \tag{11}$$

where $\overline{\left\langle I_{R+}^{(i)}\right\rangle} = \frac{1}{N}\sum_x \left\langle I_{R+}^{(i)}(x)\right\rangle$ is the average intensity of the positive image. Substituting these relations into Eq. (9), the expression for the positive image can be obtained as

$$\left\langle I_{R+}^{(i)}(x)\right\rangle = \left(\frac{\left\langle I_{B+}^{(i)}\right\rangle}{TN(1-T)} - \frac{\overline{\left\langle I_{R+}^{(i)}\right\rangle}}{1-T}\right)O(x) + \frac{\overline{\left\langle I_{R+}^{(i)}\right\rangle}}{1-T} - \frac{\left\langle I_{B+}^{(i)}\right\rangle}{N(1-T)}. \tag{12}$$

In the same way, the negative image of the object can be derived by averaging the negatively correlated speckle patterns

$$\left\langle I_{R-}^{(i)}(x)\right\rangle = \left(\frac{\overline{\left\langle I_{R-}^{(i)}\right\rangle}}{1-T} - \frac{\left\langle I_{B-}^{(i)}\right\rangle}{TN(1-T)}\right)O'(x) + \frac{\left\langle I_{B-}^{(i)}\right\rangle}{TN}, \tag{13}$$

where the subscript – denotes negative correlation, and $O'(x) = 1 - O(x)$ is the inversed object function. We note that Eqs. (12) and (13) are obtained just by statistical averaging, and are different from the previous reconstruction model of Luo *et al.*[13]. The numerical simulation results of the positive and negative images are shown in Fig. 3. The object is the same as that of Fig. 2(a). The positive and negative images retrieved just by averaging the speckle patterns separated by correlation coefficients are shown in Figs. 3(a) and (b), respectively. For the positive image, $k = 1.8166$, $\left\langle e\right\rangle = 21.3706$ in theory, and $k = 1.7603$, $\left\langle e\right\rangle = 21.4552$ in simulation. For the negative image, $k = 1.7025$, $\left\langle e\right\rangle = 19.8289$ in theory, and $k = 1.6591$, $\left\langle e\right\rangle = 19.8849$ in simulation. The numerical simulation results agree well with the above theory.

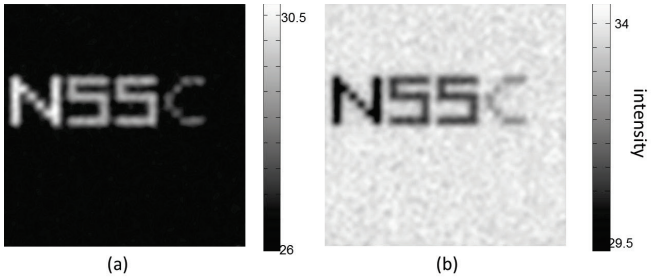

Fig. 3. Numerical simulation of CI: (a) the positive image, and $k = 1.8166$, $\left\langle e\right\rangle = 21.3706$ in theory; $k = 1.7603$, $\left\langle e\right\rangle = 21.4552$ in simulation and (b) the negative image, and $k = 1.7025$, $\left\langle e\right\rangle = 19.8289$ in theory; $k = 1.6591$, $\left\langle e\right\rangle = 19.8849$ in simulation.

For the positive image in CI, the visibility is defined as[13]

$$V_+ = \frac{\left\langle I_{R+}^{(i)}(O(x)=1)\right\rangle - \left\langle I_{R+}^{(i)}(O(x)=0)\right\rangle}{\left\langle I_{R+}^{(i)}(O(x)=1)\right\rangle + \left\langle I_{R+}^{(i)}(O(x)=0)\right\rangle}. \tag{14}$$

Substituting Eq. (12) into the above expression, we obtain

$$V_+ = \frac{\left\langle I_{B+}^{(i)}\right\rangle - NT\overline{\left\langle I_{R+}^{(i)}\right\rangle}}{(1-2T)\left\langle I_{B+}^{(i)}\right\rangle + NT\overline{\left\langle I_{R+}^{(i)}\right\rangle}}. \tag{15}$$

For a large number of measurements, we assume that

$$\left\langle \rho_{I_{R+}^{(i)}O}\right\rangle \approx \frac{\frac{1}{N}\left(\left\langle I_B^{(i)}\right\rangle - N\overline{\left\langle I_R^{(i)}\right\rangle}T\right)}{\overline{\left\langle I_R^{(i)}\right\rangle}\sqrt{{\sigma_O}^2}}. \tag{16}$$

We can see that the numerator of the visibility is related to the mean correlation coefficients of the positive patterns, namely, $\left\langle \rho_{I_{R+}^{(i)}O}\right\rangle$, so if the patterns have larger correlation coefficients, the positive image will have better visibility.

To evaluate the quality of the image, the CNR is used. For simplicity, we just consider a binary object, and assume that the variance of the noise is the same as that of the speckle pattern. Then, the CNR of the positive image should be

$$\mathrm{CNR}_+ = \frac{\left\langle I_{R+}^{(i)}(1)\right\rangle - \left\langle I_{R+}^{(i)}(0)\right\rangle}{\sqrt{2{\sigma_e'}^2}}. \tag{17}$$

Substituting Eqs. (8) and (12) into the above expression, we obtain

$$\mathrm{CNR}_+ = \frac{\sqrt{\frac{M}{2}}}{\left\langle I_{R+}^{(i)}\right\rangle}\left(\frac{\left\langle I_{B+}^{(i)}\right\rangle}{TN(1-T)} - \frac{\overline{\left\langle I_{R+}^{(i)}\right\rangle}}{1-T}\right). \tag{18}$$

Thus, the CNR of the positive image is given by

$$\mathrm{CNR}_+ = \sqrt{\frac{M}{2}}\frac{\sqrt{\sigma o^2}}{(1-T)T}\left\langle \rho_{I_{R+}^{(i)}o}\right\rangle. \tag{19}$$

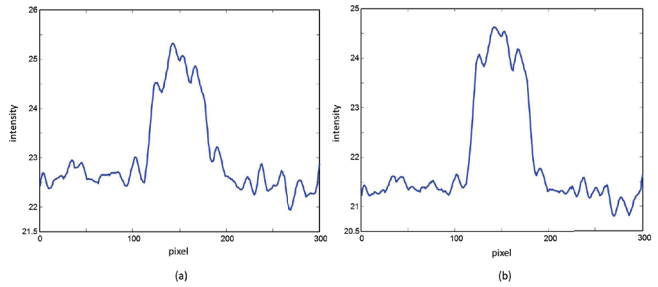

Fig. 4. Comparison between the image profiles of (a) CI and (b) correlation coefficient-based CI. The binary object is opaque except for a transparent rectangle in the center. The profile of CI with visibility 0.0422 and CNR 4.7934 is shown in (a). The profile of CI based on correlation coefficient with visibility 0.0585 and CNR 5.2397 is shown in (b).

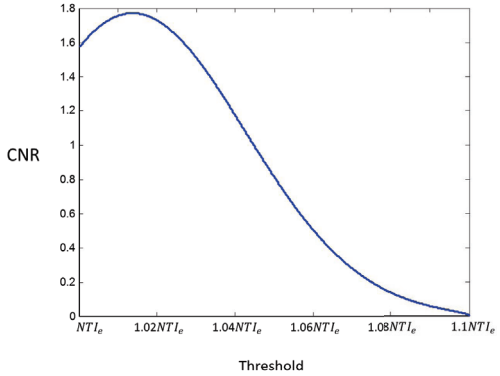

Fig. 5. Plot of CNR as a function of the threshold of the bucket detector signal.

For an object with binary transmission we have

$$\sigma_o^2 = (1 - T)\,T, \tag{20}$$

so Eq. (19) becomes

$$\mathrm{CNR}_+ = \sqrt{\frac{M}{2}}\,\frac{\left\langle \rho_{I_{R+}^{(i)} o} \right\rangle}{\sqrt{(1-T)T}}. \tag{21}$$

In Refs. [12,13], the mean of the bucket detector intensity measurements was taken as the boundary to divide the speckle patterns. A comparison between the profiles obtained by CI and correlation coefficient-based CI is shown in Fig. 4. It can be seen that the latter does indeed show improvement, with a visibility and CNR of 0.0422 and 4.7934 compared with 0.0585 and 5.2397, respectively, of the former.

To analyze the CNR of CI with a finite sampling number, we make a simplified but reasonable assumption: the intensity at each pixel is independent and identically distributed. Under this assumption and the central limit theorem, the bucket detector signals obey Gaussian distribution with the expected value NTI_e and variance NTI_e^2, where I_e is the expected intensity value at each pixel. We then have $N\overline{I_R^{(i)}T} = \left\langle I_B^{(i)} \right\rangle$, so the mean intensity of the bucket detector can be taken as the boundary to divide the speckle patterns into two parts, each part containing $M_t/2$ patterns, where M_t is the total number of speckle patterns. Then the expression for the CNR of positive image is given by

$$\mathrm{CNR}_+ = \frac{\sqrt{\frac{M_{I_B}}{2}}}{(1-T)TNI_e}\left(\frac{1}{\sigma\sqrt{2\pi}}\int_{I_B}^{NI_e} e^{-\frac{(t-\mu)}{2\sigma^2}t}\,\mathrm{d}t - NTI_e\right), \tag{22}$$

where $\mu = NTI_e$ and $\sigma^2 = NTI_e^2$, and M_{I_B} is the number of speckle patterns selected by the threshold I_B. A plot of this CNR+ as a function of the bucket detector threshold I_B, up to $1.1NTI_e$ is shown in Fig. 5, where we have taken $I_e = 20$, $M_t = 20000$, $N = 10000$, and $T = 0.2$. From the curve, we can see that we can elevate the threshold of the bucket detector signal so that we average over those speckle patterns which have larger correlation coefficients, but then the number of patterns will be reduced which will decrease the CNR. There is a maximum for CNR+ when the threshold is a little higher than the mean bucket signal, and we can see that the reconstructed image with a maximum CNR is obtained by averaging over a number of speckle patterns a little less than a half of the total.

In the same way, we can obtain the visibility and CNR of the negative image as

$$V_- = \frac{NT\overline{\left\langle I_{R-}^{(i)} \right\rangle} - \left\langle I_{B-}^{(i)} \right\rangle}{(1-2T)\left\langle I_{B-}^{(i)} \right\rangle + NT\overline{\left\langle I_{R-}^{(i)} \right\rangle}}, \tag{23}$$

$$\mathrm{CNR}_- = \frac{\sqrt{\frac{M}{2}}}{\left\langle I_{R-}^{(i)} \right\rangle}\left(\frac{\overline{\left\langle I_{R-}^{(i)} \right\rangle}}{1-T} - \frac{\left\langle I_{B-}^{(i)} \right\rangle}{TN(1-T)}\right). \tag{24}$$

A better visibility of the positive image will be achieved if the patterns have smaller correlation coefficients. There is a maximum for CNR_- when the threshold is a little lower than the mean bucket signal. The corresponding analysis will not be presented here, since it is similar to that for the positive image and would not add much insight.

In conclusion, we present a newly modified nonlocal imaging technique called CI based on correlation coefficients, in which the correlation coefficient is utilized to separate the speckle patterns into positive and negative correlated parts. The positive and negative images of the object are obtained just by averaging the respective speckle patterns. In this method, only less than a half of the total speckle patterns need to be used to obtain a maximum CNR. Compared with conventional GI, the computation time is greatly reduced, which is a particular advantage when the images are large. It is hoped that this correlation coefficient-based CI technique may be incorporated into real applications.

The authors thank Kai-Hong Luo and Ling-An Wu for helpful discussions. This work was supported by the National Natural Science Foundation of China under Grant No. 61274024.

References

1. T. B. Pittman, Y. H. Shih, D. V. Strekalov, and A. V. Sergienko, Phys. Rev. A **52,** R3429 (1995).
2. R. S. Bennink, S. J. Bentley, R. W. Boyd, and J. C. Howell, Phys. Rev. Lett. **92,** 033601 (2004).
3. J. Cheng and S. Han, Phys. Rev. Lett. **92,** 093903 (2004).
4. A. Gatti, E. Brambilla, M. Bache, and L. A. Lugiato, Phys. Rev. Lett. **93,** 093602 (2004).
5. D. Z. Cao, J. Xiong, and K. Wang, Phys. Rev. A **71,** 013801 (2005).
6. D. Zhang, Y. H. Zhai, L. A. Wu, and X. H. Chen, Opt. Lett. **30,** 2354 (2005).
7. D. Duan and Y. Xia, Chin. Opt. Lett. **10,** 031102 (2012).
8. Y. Zhang, J. Shi, H. Li, and G. Zeng, Chin. Opt. Lett. **12,** 011102 (2014).
9. J. H. Shapiro, Phys. Rev. A **78,** 061802(R) (2008).
10. F. Ferri, D. Magatti, L. A. Lugiato, and A. Gatti, Phys. Rev. Lett. **104,** 253603 (2010).
11. J. Du, W. L. Gong, and S. S. Han, Opt. Lett. **37,** 1067 (2012).
12. L. A. Wu and K. H. Luo, AIP Conf. Proc. **1384,** 223 (2011).
13. K. H. Luo, B. Q. Huang, W. M. Zheng, and L. A. Wu, Chin. Phys. Lett. **29,** 074216 (2012).
14. R. E. Meyers, K. S. Deacon, and Y. H. Shih, Appl. Phys. Lett. **100,** 131114 (2012).
15. M. F. Li, Y. R. Zhang, K. H. Luo, L. A. Wu, and H. Fang, Phys. Rev. A **87,** 033813 (2013).
16. K. W. C. Chan, M. N. O'Sullivan, and R. W. Boyd, Opt. Express **18,** 5562 (2010).
17. W. V. Nicholson, IEEE Trans. Bio. Med. Eng. **51,** 2006 (2004).
18. J. W. Goodman, *Speckle Phenomena in Optics: Theory and Applications* (Roberts, 2006).